

Manuscript submitted March 4, 1991; revised manuscript received April 30, 1991.

REFERENCES

1. Z. H. Walker and E. A. Ogryzlo, *J. Chem. Soc. Faraday Trans.*, **87**, 45 (1991).
2. E. A. Ogryzlo, D. L. Flamm, D. E. Ibbotson, and J. A. Mucha, *J. Appl. Phys.*, **64**, 6510 (1988).
3. H. F. Winters and D. Haarer, *Phys. Rev. B*, **36**, 6613 (1987).
4. E. A. Ogryzlo, D. E. Ibbotson, D. L. Flamm, and J. A. Mucha, *J. Appl. Phys.*, **67**, 3115 (1990).
5. Z. H. Walker and E. A. Ogryzlo, *ibid.*, **69**, 2635 (1991).
6. Z. H. Walker and E. A. Ogryzlo, *ibid.*, **69**, 548 (1991).
7. Z. H. Walker and E. A. Ogryzlo, In press, *Chem. Phys.* (1991).

Optimization and Characterization of LPCVD TiB₂ for ULSI Applications

C. S. Choi* and G. A. Ruggles**

Department of Electrical and Computer Engineering, North Carolina State University, Raleigh, North Carolina 27695

C. M. Osburn**

Department of Electrical and Computer Engineering, North Carolina State University, Raleigh, North Carolina and MCNC, Center for Microelectronics, Research Triangle Park, North Carolina 27709

G. C. Xing*

Department of Material Science and Engineering, North Carolina State University, Raleigh, North Carolina 27695

ABSTRACT

The chemical vapor deposition of TiB₂ from gaseous mixtures of TiCl₄, B₂H₆, and H₂ onto various substrates was studied. A thermodynamic analysis using the SOLGASMIX computer program indicated that at an input gas ratio corresponding to the stoichiometry of TiB₂, the amount of secondary-phase deposition would be considerably reduced compared to that of TiB₂. For nonstoichiometric input gas mixtures, other solid phases, including oxides and silicides, are expected to result from the reaction with substrates. Experimental depositions of films were carried out in a cold wall system over a broad range of temperatures, pressures, and input gas flow rates. X-ray diffraction and x-ray photoelectron spectroscopy data indicate that the as-deposited films are very fine grained polycrystalline or amorphous, and the films RTA-annealed above 900°C are crystalline TiB₂. Below 550°C, surface reactions are the dominant factor for the kinetics of TiB₂ deposition, while mass transport is a limiting step for deposition above 550°C. At higher temperatures the deposition rate increases linearly with flow rate and total pressure, suggesting the deposition mechanism is reactant limited. The B/Ti ratio determined via Auger electron spectroscopy approaches the stoichiometric value of two in higher temperature films, while the presence of excess boron and chlorine was detected for low-temperature films. Stoichiometric TiB₂ films were deposited over a wide range of input gas mixture B/B+Ti ratios ranging from 0.4 to 0.71. Depletion effects of input gas were observed at low flow rate and high pressure where the residence time of reactants is longer than 10 s.

As the device density of a semiconductor chip increases in each generation, the feature sizes, both lateral and vertical, decrease according to scaling theory. However, there are several components that deviate from scaling theory inherently. In particular, the thickness of the metal interconnection typically cannot be fully scaled down because of the resistivity and electromigration limitations of currently used materials such as polysilicon and aluminum. Even with full scaling, the interconnection RC time constant remains invariant and can become dominant as the raw device delay is reduced by geometric device scaling. For gate level interconnection, the most widely used material is polycrystalline silicon, but its high resistivity places a potentially severe limit on its performance in very large scale integrated applications. Furthermore, with the concomitant reduction of junction depth and contact hole size, the interaction between the contact metallurgy and the underlying semiconductor is a serious problem, because the interaction may lead to junction shorting or to high contact resistance. High series or contact resistance to ultrashallow junctions can also severely limit overall device performance (1). Hence, it has been necessary to develop new metallization materials (2) with improved contact and barrier characteristics, as well as with high conductivity.

Because of its interesting properties, titanium diboride has been investigated and commercially used for several applications such as: crucible materials for melting metals,

thermocouple protection tubes in melting metal, abrasives, protective coatings, high-temperature electrodes in nuclear fusion applications, and cathodes or containers in aluminum reduction cells. Nicolet (3) has already pointed out titanium boride as an interesting potential material for microelectronic device fabrication. The high conductivity and chemical inertness at high-temperature leads TiB₂ to be considered as a potential candidate for a diffusion barrier or gate/diffusion cladding. The resistivity of bulk polycrystalline TiB₂ ($\approx 10 \mu\Omega\text{-cm}$) (4) and single crystal ($6 \mu\Omega\text{-cm}$) (5) is lower than that of other potential barrier materials like silicides or nitrides and only slightly higher than that of tungsten. Shappirio *et al.* showed that ZrB₂ is stable in contact to aluminum up to 600°C (6). Feldman *et al.* used TiB₂ as an electrode in polycrystalline silicon thin film solar cells (7).

Several different methods have been employed to produce TiB₂ thin films: *i.e.*, sputtering (6, 8-12), reactive ion plating (13), laser induced vapor-phase synthesis (14), and reaction of Ti-B thin film couples (15). Due to stringent ultra large scale integrated (ULSI) requirements for low thermal budget, conformal step coverage, and high-purity films, low pressure chemical vapor deposition is a good choice for producing high quality TiB₂ films.

Chemical vapor deposited (CVD) polycrystalline TiB₂ films have been initially obtained from a source gas of TiCl₄/BCl₃/H₂. Peshev and Niemyski (16) deposited TiB₂ films in the temperature range of 1000-1400°C. A pyrolytic deposition of TiB₂ was performed (17, 18) at 1400-1600°C and at 3-5 torr. Models for the deposition process were de-

* Electrochemical Society Student Member.

** Electrochemical Society Active Member.

Table I. Phases deposited on different substrates as simulated using SOLGASMIX at 350-800°C at 1 torr as a function of input gas ratio.

Substrate	$B_2H_6/TiCl_4$ ratio in input gas mixture			
	$TiCl_4$ only	$TiCl_4$ rich	1:1	B_2H_6 rich
None ^a	None, $TiCl_3^b$	TiB_2	TiB_2	TiB_2 , B
Si	$TiSi$, $TiSi_2^b$	$TiSi$, TiB_2^c	TiB_2	B, TiB_2^c
SiO_2	Ti_2O_3 , $Ti_5Si_3^d$	TiB_2 , $Ti_2O_3^c$ B_2O_3	TiB_2 $B_2O_3^{b,c}$ $Ti_2O_3^c$	TiB_2 , B, $B_2O_3^b$
TiB_2	None, $TiCl_3^b$	TiB_2	TiB_2	TiB_2 , B
$TiSi_2$	$TiCl_3^b$, $TiSi$	$TiSi$, TiB_2	TiB_2 , $TiSi$, Si	TiB_2 , Si, B
Ti	$TiCl_3^b$	TiB_2	TiB_2	TiB_2
B	TiB_2	TiB_2	TiB_2 , B	B, TiB_2

^a A hypothetical inert substrate.

^b Deposit or form only at low temperature.

^c One order of magnitude smaller than primary phase.

^d Deposit or form only at high temperature.

veloped based on the experimental results of deposition rates and efficiencies (19), coupled with thermodynamic calculations for CVD TiB_2 . Pierson and Mullendore (20) reported that the atmospheric CVD at 900-950°C produced boron-rich titanium diboride even at a stoichiometric input gas. A deposition study combined with a thermodynamic study suggested that equilibrium is approached under typical TiB_2 CVD conditions, and that the deposited phases are far more sensitive to changes in system chemistry than they are to changes in temperature (21). A glow discharge deposition (22) was performed at temperatures from 480 to 650°C, resulting in as-deposited resistivity ranging from about 200-450 $\mu\Omega\text{-cm}$. A chemical vapor deposition of titanium diboride using the reaction of $TiCl_4$ with B_2H_6 in a hydrogen atmosphere in the temperature range of 600-900°C temperature was also reported (23). The deposition rate of the B_2H_6 reaction was considerably greater than that of the BCl_3 reaction, and it proceeded at a lower temperature; however, the deposition rate was negligible below 700°C, and above 1000°C the deposition tended to be powdery, probably the result of vapor-phase nucleation.

This work consists of both a through thermodynamic analysis of the deposition of TiB_2 films via CVD, as well as specific experimental results for the mechanism of TiB_2 film deposition at various temperatures, pressures, gas mixtures, and flow rates.

Thermodynamic Analysis

The calculation of equilibrium states in a chemical system is an important step towards the design of processes involving chemical reactions. A thermodynamic study is typically used as a guide to determine the effects of changing the controllable experimental variables such as temperature, total pressure, and the ratio of the chemical elements in the input gas ratio on the deposited film properties. An initial attempt to analyze the thermodynamics for CVD of TiB_2 was made by Peshev and Niemyski (16), and a more extensive thermodynamic analysis of deposition from gaseous $TiCl_4$, BCl_3 , and H_2 was conducted by Besmann and Spear (19). In the absence of substrate reactions, TiB_2 and boron are the only solid phases which can be deposited. The theoretical efficiency of deposition appeared to generally increase with increasing temperature, decreasing Cl/Cl + H fraction in the reactant gas, and decreasing total pressure. Randich and Gerlach (21) used the quaternary-phase diagram to determine bulk compositions and phase fields accessible by CVD techniques. They found that the accessible region of the quaternary phase diagram of Ti-B-Cl-H is very limited, i.e., it is not thermodynamically possible to obtain titanium or TiB using $TiCl_4$ and BCl_3 source gas, and the predicted deposit in the accessible area is only TiB_2 or $TiB_2 + B$.

In this work, a thermodynamic analysis of the chemical vapor deposition of TiB_2 from gaseous $TiCl_4$, B_2H_6 , and H_2 was performed using SOLGASMIX, which determines the equilibrium mixture by minimizing the total Gibbs free energy of the system. To be more realistic, interactions between input gases and the substrate were also investi-

gated, and are summarized in Table I. The inclusion of the substrate in the calculations results in the possible formation of solid phases brought about via reaction between the gas and the substrate, rather than deposition. This is the case for titanium silicide formation on a Si substrate, and the formation of oxides of boron and titanium on an SiO_2 substrate. Although the production of such phases would indeed be problematic, in most cases, such reactions would be expected to be self limiting, due to the continual requirement for substrate material to interact with gas ambient via interdiffusion through the film.

Deposition on inert or TiB_2 substrate.—A TiB_2 substrate is predicted by SOLGASMIX to be inert to an input gas mixture of $TiCl_4$, B_2H_6 , and H_2 at least up to 800°C. According to the calculated results, $TiB_2(s)$, HCl , BCl_3 , $BHCl_2$, and $TiCl_3$ are the major new products in the temperature range of 400-800°C (Fig. 1). The B_2H_6 reactant that is introduced into a system almost completely reacts with chloride from $TiCl_4$ to form BCl_3 , resulting in a partial pressure of B_2H_6 that is extremely low ($\leq 10^{-20}$ atm). As seen by the decreasing partial pressure of the boron containing species ($BCl_3 + BHCl_2$) and the dominant titanium containing species ($TiCl_4$) decrease at higher temperature, the deposition efficiency of TiB_2 is greater at higher temperature. The window for single-phase TiB_2 deposition is as wide as $0 < B/B + Ti < 0.8$ for deposition temperatures below 800°C, but boron is deposited for $B/B + Ti \geq 0.8$. The deposition of $TiCl_3$ is predicted by the H_2 reduction of $TiCl_4$, and it deposits at low temperatures ($\leq 350^\circ\text{C}$) for an input gas of $TiCl_4$ and H_2 .

Deposition on Si substrate.—The equilibrium analysis of TiB_2 deposition on silicon substrates, i.e., Ti-B-Cl-H-Si system, was carried out, and Fig. 2 illustrates the equilibrium partial pressures of gaseous species calculated from an input gas mixture with $B/B + Ti = 0.67$ as a function of

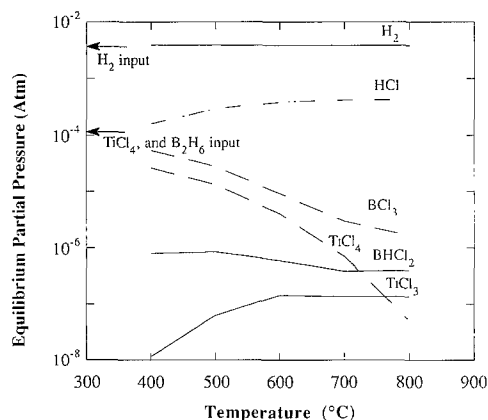


Fig. 1. The equilibrium partial pressures of the gaseous species calculated for chemical vapor deposition of TiB_2 from $TiCl_4$, B_2H_6 , and H_2 on an inert substrate with an input gas mixture of $B/B + Ti = 0.67$ at various temperatures.

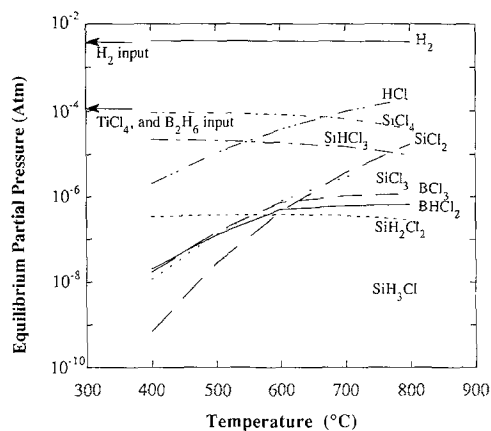


Fig. 2. The equilibrium partial pressures of the gaseous species calculated for chemical vapor deposition of TiB_2 from $TiCl_4$, B_2H_6 , and H_2 on a Si substrate with an input gas mixture of $B/B + Ti = 0.67$ at various temperatures.

temperature. It indicates that H_2 , HCl , $SiHCl_3$, $SiCl_4$, $SiCl_3$, $SiCl_2$, and BCl_3 are the major gaseous species at equilibrium. The titanium is almost completely deposited as evidenced by the very low partial pressures ($\leq 10^{-10}$ atm) of titanium chlorides ($TiCl_x$). The molar ratio of deposited TiB_2 to total deposited secondary phases, i.e., $B + TiSi_2$, at various temperatures is illustrated as a function of reactant gas ratio in Fig. 3 for a silicon substrate. The production of $SiH_xCl_y(g)$ (Fig. 2) may indicate that $TiCl_4$ is almost completely reduced by Si. From $TiCl_4$ -rich input gas mixtures, multiphase deposits of titanium silicides and titanium diboride are predicted. From diborane-rich input gas mixtures, almost all the titanium in the system reacts to produce titanium diboride, leaving the partial pressure of species containing titanium extremely low ($< 10^{-11}$ atm) and that of BCl_3 extremely large. Thus, elemental boron is predicted to accompany the TiB_2 deposition. However, at an input gas ratio corresponding to the stoichiometry of TiB_2 , the amount of secondary-phase deposition is considerably reduced compared to that of TiB_2 . At $600^\circ C$, a film impurity level of one part per thousand is expected; while films deposited at $700^\circ C$ would contain only 100 ppb of unwanted secondary phases. Hence the permissible range of input gas ratios needed to deposit only TiB_2 increases with increasing temperature.

Deposition on SiO_2 substrates.—The equilibrium partial pressures of gaseous species in a chemical system of Ti-B-Cl-H-Si-O (for the case of an SiO_2 substrate) are shown as a function of temperature in Fig. 4. As temperature increases, the partial pressure of HCl increases and those of BCl_3 , $TiCl_4$, and H_2 decrease, indicating efficient deposition of TiB_2 at high temperature. SOLGASMIX predicts

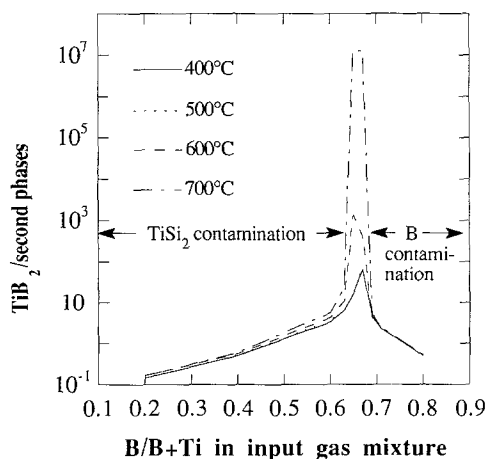


Fig. 3. Thermodynamic calculation of the ratio of TiB_2 deposition to secondary-phase deposition on a Si substrate at various temperatures.

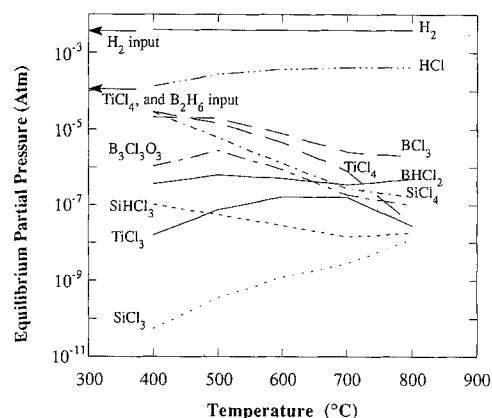


Fig. 4. The equilibrium partial pressures of the gaseous species calculated for chemical vapor deposition of TiB_2 from $TiCl_4$, B_2H_6 , and H_2 on an SiO_2 substrate with an input gas mixture of $B/B + Ti = 0.67$ at various temperatures.

that silicon dioxide reacts with a chlorine containing species to produce volatile silicon chlorides, $SiCl_4$, $SiHCl_3$, and that titanium oxide is thereby formed under these input gas ratios. Figure 5 shows the ratio of TiB_2 to secondary deposits on silicon dioxide substrates as a function of input gas ratio at various deposition temperatures. In addition to TiB_2 , titanium oxides or boron oxides ($\leq 400^\circ C$) are expected to deposit on SiO_2 substrates in a $TiCl_4$ -rich gas mixture while boron, titanium diboride, and boron oxides ($\leq 400^\circ C$) are expected in a B_2H_6 -rich gas mixture. Due to a significant amount of B_2O_3 formation at low temperatures, and B deposition at high temperatures, the window for nearly pure TiB_2 is the widest at $600^\circ C$, where a film impurity of only 100 ppb is expected.

To take advantage of the widest single-phase window possible for the Si and SiO_2 substrates, the thermodynamically optimized standard condition for input gas mixture and deposition temperature were chosen as; $B/B + Ti = 0.67$ and $600^\circ C$, respectively.

Deposition on $TiSi_2$, Ti, or B substrates.—For an input gas of $TiCl_4 + H_2$, and a Ti substrate, SOLGASMIX predicts that $TiCl_3$ deposits at low temperature ($\leq 400^\circ C$). Above $400^\circ C$, the $TiCl_3$ is volatile, and a net etching of the Ti substrate occurs. The $TiCl_3$, either in gas phase or solid, is formed presumably both by a disproportionation reaction of $TiCl_4$ in the presence Ti (s), and by a hydrogen reduction of $TiCl_4$. For the input gas mixture $B/B + Ti > 0$, some Ti is supplied from the substrate to form TiB_2 , resulting in an etching of the Ti substrate. Therefore, pure TiB_2 could be produced even in a boron-rich gas mixture, and

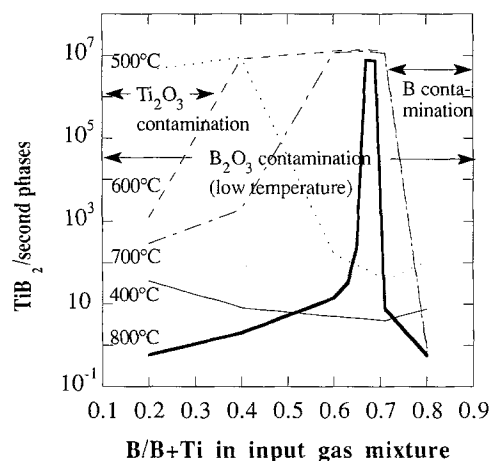


Fig. 5. Thermodynamic calculation of the ratio of TiB_2 deposition to secondary-phase deposition on an SiO_2 substrate at various temperatures.

the deposition of elemental B is predicted only for a pure diborane input gas.

In case of a boron substrate, TiB_2 is deposited even for pure TiCl_4 inputs, indicating that the boron substrate acts as a supplier of B. The concurrent deposition of B and TiB_2 takes place for the input gas mixture $\text{B/B} + \text{Ti} \geq 0.63$ at 800°C and 0.71 for 400°C .

The reaction of a TiSi_2 substrate and the reactant gases is very significant. No window for deposition of single-phase TiB_2 is found in the temperature range of $400\text{--}800^\circ\text{C}$. For an input gas of TiCl_4 and H_2 , titanium disilicide transforms to a higher titanium silicide (TiSi) during deposition at the temperature range studied. The amount of titanium in titanium silicide increases, while that of silicon in titanium silicide decreases. In other words, additional Ti deposits from the gas phase to form a higher silicide, and Si in the silicide is etched. For titanium-rich gas mixtures, concurrent titanium diboride deposition, and titanium silicide-phase formation is expected. As more diborane is introduced in the input gas mixture, the amount of deposited TiB_2 increases, and Si starts to segregate and etch due to a decomposition of TiSi_2 . At a boron-rich input gas mixture, titanium silicide is completely consumed, leaving Si and elemental B deposits.

Experimental

The low-pressure chemical vapor deposition reactor, depicted schematically in Fig. 6, consists of a deposition chamber, gas distribution system, heating system, and pumping system. The overall reaction chamber is made up of a cylindrical high purity 316 stainless steel chamber penetrated by various ports, feedthroughs, and windows. The substrate is heated in the center of the chamber by means of a pyrolytic boron nitride-coated graphite heating element. The heater employs closed loop temperature control using a thermocouple mounted within a graphite susceptor on top of the element and is capable of heating the substrate to approximately 1000°C . High-purity gases are brought to the reaction chamber in stainless steel tubing using VCR fittings for ultimate vacuum integrity. The gases are introduced just above, and parallel to, the substrate to help promote uniform film growth. The reactant gases used for deposition of titanium diboride are TiCl_4 (Alfa, 99.999%), 10% B_2H_6 in H_2 (Voltaix), and H_2 (Airco). TiCl_4 is a liquid at room temperature; therefore the source cylinder of TiCl_4 is maintained at $\approx 60^\circ\text{C}$ which keeps its vapor pressure above 70 torr (24). The flow of the vapor of TiCl_4 is controlled by a high-temperature mass flow controller, maintained at 90°C , without using an additional carrier gas. The lines of the TiCl_4 cylinder are differentially heated with heating tapes, resulting in a temperature gradient, maintained from the TiCl_4 source to the mass flow controller, which prevents TiCl_4 vapor from condensing in the line. The chamber is pumped by a 510 liter/s corrosive service turbomolecular pump, which is backed by a 1520 liter/min corrosive service rotary vane mechanical

pump. This combination provides sufficient pumping speed at the expected process pressures as well as a good initial base pressure. Gate valves isolate the chamber, turbo pump, and backing pump. The pressure is monitored by a capacitance manometer at high pressure ($>10^{-3}$ torr) and by an ion gauge at low pressure ($<10^{-3}$ torr). The deposition pressure is controlled by an automatic throttle valve coupled to a capacitance manometer.

Titanium boride films were deposited on bare Si, or thermally oxidized silicon wafers. Chemical vapor deposition of TiB_2 for this work was done over a wide range of process temperatures ($375\text{--}750^\circ\text{C}$), pressures (0.5-5 torr), and total flow rates (69-550 sccm). The $\text{B/B} + \text{Ti}$ ratio of the input gases was varied from Ti rich ($\text{B/B} + \text{Ti} \approx 0$) to B rich ($\text{B/B} + \text{Ti} \approx 1$). Only one parameter was varied for each set of experiments, while the others were held at a nominal value.

The deposition procedure commenced with loading of a 100 mm silicon wafer with a 450 nm thermal oxide into the deposition chamber. The base pressure prior to wafer loading was usually mid 10^{-7} torr. After pumping on the chamber for about 1 h to reduce the base pressure to 10^{-6} torr, the heater was turned on, and H_2 was introduced at the same flow rate as the total of the TiCl_4 , B_2H_6 , and H_2 to stabilize the throttle valve at the process pressure. Once the wafer temperature approached the deposition temperature, the input gases were allowed to flow through bypassed lines of the three-way valves, connected to the backing pump for about 30 s. After both temperature and flow rates stabilized, the reactant gases were introduced into the chamber by changing the path of the three-way valves. The three-way valves were installed at the same distance from the chamber so that the input gases reach the substrate at the same time. At the end of deposition, the flow of B_2H_6 and TiCl_4 were simultaneously terminated, and the heater was turned off. Then, H_2 was introduced and the throttle valve was opened all the way to purge out the reactants quickly and to help cool the wafer. The TiCl_4 line and its mass flow meter were purged and pumped out through a by-pass line after each run. Nitrogen was used to vent the chamber to unload a wafer.

The thicknesses and surface roughness of the TiB_2 films were measured using a Dektak profilometer after etching through the film with a 30% H_2O_2 solution at room temperature for 1-10 min to provide a step at the measurement point. The thickness of some samples was verified using Rutherford backscattering spectroscopy (RBS) and/or cross-sectional transmission electron microscopy (TEM). The thickness of films deposited below 600°C was measured via angle lapping and cross sectional SEM. The composition and phases of the films were determined by Auger electron spectroscopy (AES), x-ray photon spectroscopy (XPS), and x-ray diffraction.

The optimized deposition conditions were achieved through a careful characterization of the as-deposited and annealed TiB_2 films. This optimization required measuring the following parameters: phases and crystallinity, stoichiometry, resistivity, impurity incorporation into the films, deposition rate, and uniformity. The application of TiB_2 as a diffusion barrier, and its stability to Al or to Cu is discussed in detail elsewhere (25).

Results and Discussion

Film chemistry.—X-ray diffraction was employed to identify the phases present in the as-deposited films. No x-ray diffraction lines of TiB_2 were observed at a deposition temperature up to 750°C , suggesting the presence of a very fine grained polycrystalline or amorphous phase for the as-deposited films. As shown in Fig. 7, the films RTA-annealed above 900°C gave patterns corresponding to the TiB_2 structure, and the intensities of the TiB_2 peaks increased as the annealing temperature was increased. The x-ray data indicated that the average grain size in TiB_2 film grows with annealing temperature. Only the as-deposited sample showed a silicon substrate line, which is probably due to a stress buildup during film deposition. The grain-size growth and the resistivity reduction with annealing temperature are discussed in detail elsewhere (26). In addition, XPS, coupled with depth profiling, was performed to

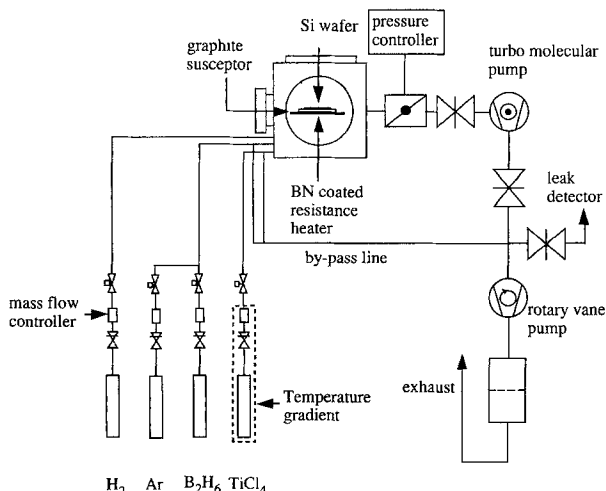


Fig. 6. Experimental apparatus for TiB_2 deposition.

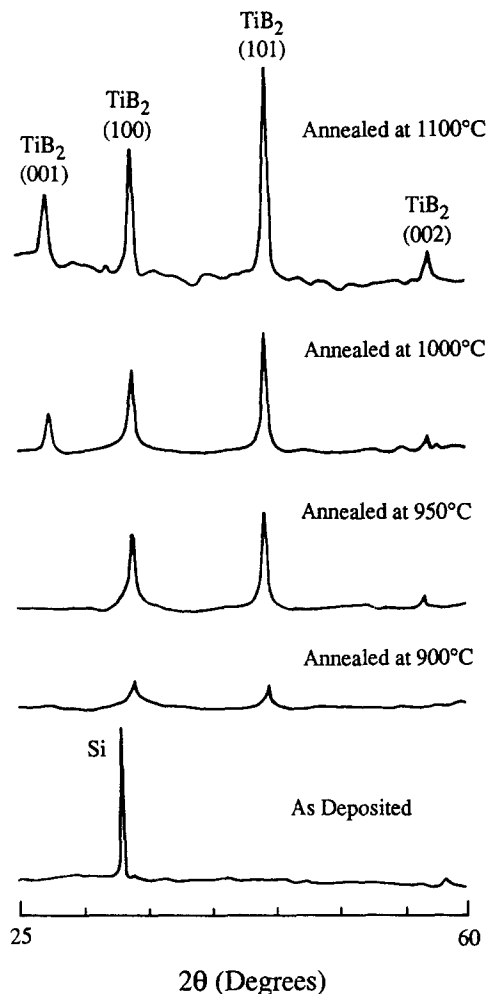


Fig. 7. X-ray diffraction patterns of TiB₂ for as-deposited and annealed films.

find the phase(s) and chemical composition of the films. A typical result for a stoichiometric TiB₂ film deposited at 650°C and 5 torr is shown in Fig. 8. No phase and composition change in the bulk film were noticed after rapid thermal anneal at 1150°C, 10 s (27). The film appears to be pure

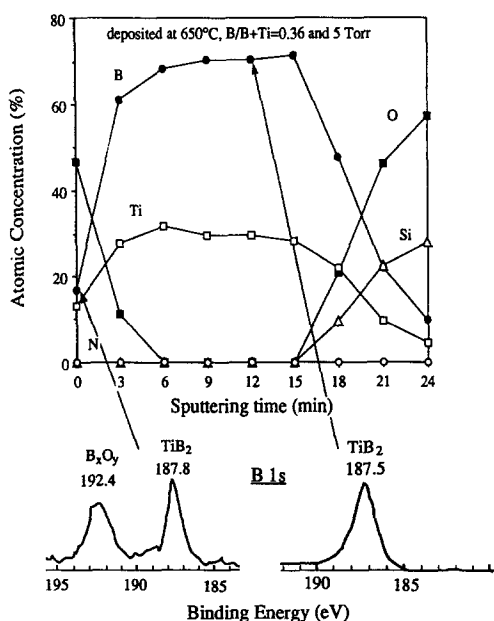


Fig. 8. XPS depth profiling and binding energy for as-deposited TiB₂ films.

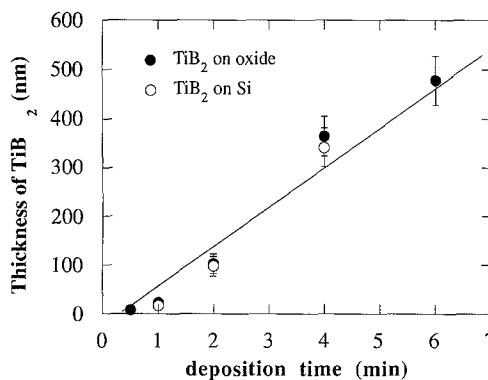


Fig. 9. The thickness of TiB₂ films as a function of deposition time. The TiB₂ films were deposited on silicon dioxide substrates or silicon substrates at 600°C, 1 torr, B/B + Ti = 0.67, TiCl₄ 25 sccm, and 10% B₂H₆ in H₂ 250 sccm.

TiB₂, with some oxygen present only at the surface, presumably due to surface oxidation. Examination of the B 1s peak in detail revealed that only Ti—B bonding was present in the film, with the exception of the surface, where some B—O bonding is also present, revealing the formation of B_xO_y.

The effect of deposition time on deposition rate.—The dependence of the film thickness on the deposition time was examined in Fig. 9. The TiB₂ films were deposited on silicon, or thermal oxide substrates under a typical deposition condition: 600°C, 1 torr, TiCl₄ = 25 sccm, and 10% B₂H₆ in H₂ = 250 sccm (B/B + Ti = 0.67). The film thickness increased linearly with the growth time, and the deposition rate was independent of the substrate (Si vs. SiO₂). Some evidence of an incubation time (≈20 s) was observed. Since this time is very small compared to a typical deposition time (6 min), the growth rate was calculated simply by dividing the film thickness by the growth time in this work.

The effect of temperature on the deposition.—The effect of temperature on deposition rate of TiB₂ was studied as shown in Fig. 10. The depositions of TiB₂ were done at 3 torr, B/B + Ti = 0.67 in the temperature range of 375–750°C. This graph contains an Arrhenius plot of the logarithm of the deposition rate as a function of reciprocal temperature. As can be seen in this figure, two distinct regimes

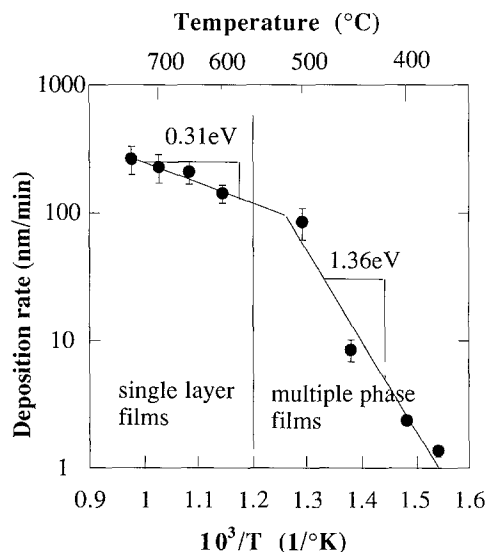


Fig. 10. Deposition rate of titanium diboride films as a function of temperature. The activation energy of TiB₂ deposition is 0.31 eV above 600°C, and 1.38 eV below 600°C. The depositions were performed at 3 torr, B/B + Ti = 0.67, TiCl₄ 25 sccm, 10% B₂H₆ in H₂ 250 sccm, and H₂ 625 sccm.

of deposition kinetics are evident. From standard CVD theory, the presence of the two regimes is defined by the type of controlling reaction rate; if the surface reaction is rate limiting, as is often the case at low temperature, the deposition rate will be a strong function of deposition temperature. If the rate limiting step is either reactant limited or diffusion controlled, the temperature dependence will be slight. As can be seen from the figure, below 550°C surface reactions are apparently the dominant factor for the kinetics of TiB_2 deposition, while mass transport is a limiting step for deposition above 550°C. Activation energies for deposition are 1.36 and 0.31 eV for low and high temperature deposition, respectively. The reported value of the activation energies for TiB_2 deposition from BCl_3 , TiCl_4 , and H_2 source were 1.74 and 0.17 eV (28).

Figure 11 shows the B/Ti and the Cl/Ti mole ratios as a function of deposition temperature. The B/Ti ratio of films was determined by AES coupled with depth profiling. A 3 keV Ar beam was used for sputtering the film. The lack of a titanium diboride standard did not allow us to calibrate the B/Ti ratio precisely. Instead, the sensitivity factors of metallic titanium and metallic boron were adopted to quantify the ratio. AES analysis of the film indicated the presence of excess boron throughout the bulk for films deposited at low temperatures. For example, the B/Ti ratio for a TiB_x film deposited at 500°C was found to be 2.6 rather than the 2.0 value obtained for higher deposition temperatures. In addition, during wet etching, the films deposited at temperatures below 600°C, could not be completely removed. The residual layer, which was not completely etched in H_2O_2 , is believed to result from concentration of a boron phase as the boron-rich titanium boride film is etched, ultimately resulting in a layer which resists further etching. Thus, thickness data were obtained from cross-sectional SEM after an angle lapping. As the deposition temperature increases, the B/Ti ratio approaches the stoichiometric value of 2, within the reasonable uncertainty of the AES sensitivity factors, and stays constant at higher temperatures. Pierson and Mullendore (23) also found boron-rich films deposited at 600°C or below and more stoichiometric films at higher temperature. In addition to the problem of excess boron, a large Cl content was observed in low temperature films as well. At 600°C and above the Cl was at the detection limit for energy dispersive spectroscopy (2%). The decomposition of the chlorides at lower temperature is presumably not efficient, so that the films containing chlorine and excess boron are deposited. The benefit of higher temperature deposition in producing purer and more stoichiometric films is clear, and qualitatively in agreement with the thermodynamic calculations.

The effect of input gas mixture on deposition.—The deposition rate of titanium boride films was measured for the films deposited at 600°C, 3 torr for 6 min. The B/B + Ti ratio of the input gas mixture was varied from 0.0 to 0.8 at a constant total flow rate of 550 sccm. In the temperature range 375–750°C, a violet-colored film was deposited on the cold wall and the color changed to white when the cham-

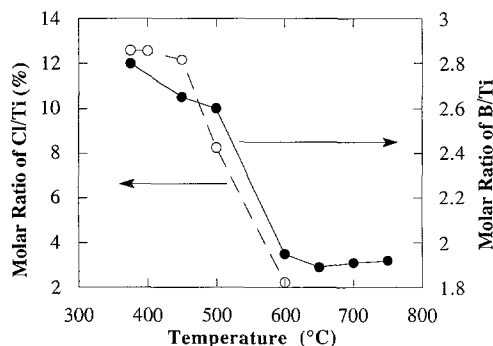


Fig. 11. The B/Ti and Cl/Ti ratio in the titanium boride films deposited on SiO_2 as a function of deposition temperature. The depositions were performed at B/B + Ti = 0.67, 1 torr.

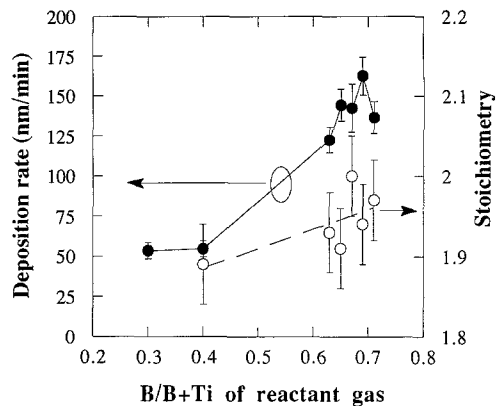


Fig. 12. Input gas ratio dependence of deposition rate and stoichiometry (B/Ti ratio) for TiB_2 films. The films were deposited at 600°C, 3 torr, and the B/Ti ratio was measured by AES.

ber door was opened. The deposition on the wall was more pronounced in lower total pressure runs, in which the deposition efficiency is lower. It is believed that the observed films were titanium subchloride(s) because both TiCl_3 (22, 29, 30) and TiCl_2 (23) are reported as stable substances below 440 and 475°C, respectively.

One interesting observation is the reaction between a Si substrate and the reactant gas in a CVD system containing only TiCl_4 (B/B + Ti = 0), since TiSi_2 could form. In this work, no discernible depositions were observed when 75 sccm of TiCl_4 and 925 sccm of H_2 were introduced at either 375 or 600°C, 3 torr for 20 min. Reynolds *et al.* also found no reaction at 627°C when TiCl_4 was introduced over a Si wafer; however, he did form TiSi_2 , and simultaneously etch Si above 827°C over the pressure range of 1–750 mtorr (31). Bouteville *et al.* used a hydrogen reduction of TiCl_4 in the temperature range of 700–1000°C and a total pressure of 0.75 torr to form titanium silicide selectively on Si (32).

The deposition rate and B/Ti atomic ratio determined via AES are plotted as a function of the B/B + Ti ratio in the reactant gas mixture in Fig. 12. The B/Ti ratio and the deposition rate were found to be dependent on the input gas ratio. No deposition is observed at an input gas mixture of B/B + Ti = 0 (TiCl_4 only). On the other hand, the films deposited at B/B + Ti = 0.8 were very nonuniform in composition and color. For this boron-rich input gas mixture, the B/Ti ratio in the film increases from 2.4 to 9.9 along the direction in which the input gases travel, indicating a depletion of TiCl_4 . The peak in deposition rate occurs close to an input gas ratio corresponding to stoichiometry (0.67). Such a peak in deposition rate from a fixed total flow system could be expected from a highly efficient, or reactant-limited process. However, it is difficult to conclude whether there is a true maxima in the B/Ti ratio at B/B + Ti = 0.67 in the input gas, or if the data represent noise in the AES measurements. The films were found to have a constant, nearly stoichiometric B/Ti ratio over a wide range of input gas mixture ratios ranging from 0.4 to 0.71. This result indicates that the window to deposit a single phase TiB_2 with very limited amount of secondary deposits (*e.g.*, <0.1%) was wide, as predicted by thermodynamic calculations (*e.g.*, 600°C in Fig. 5).

The effect of input gas flow rate on deposition.—The deposition rate at 600°C increases linearly with total flow rate, from 70 to 550 sccm, as shown in Fig. 13. However the TiB_2 thickness (deposition rate) also varies along the gas flow direction as shown in Fig. 14. For flow rates below 140 sccm, the thickness of the film decreases monotonically along the substrate in the direction of gas travel; at higher flow rates the film thickness maximum moves toward the center of the wafer.

For the transport of gaseous species between the bulk gas and the deposition surface, it is usually assumed that a laminar boundary layer lies between the turbulent bulk gas flow and the deposition surface, and that the diffusion of gaseous species through the laminar boundary layer is a

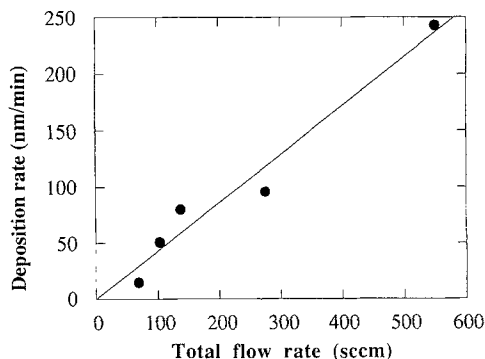


Fig. 13. Deposition rate as a function of total flow rate. The deposition rate increases linearly with flow rate. The depositions were performed at $B/B + Ti = 0.67$, $600^\circ C$, and 1 torr.

possible rate-limiting step. Typically two distinct types of mass transport limitations are associated with reactant flux into the reaction chamber, and the combination of these two establishes the mass transport limiting aspects of a reaction taking place in a given open tube system. The first depends entirely on the rate of introduction of gaseous reactant into the chamber. The second depends on the movement of this introduced mass to all portions of the reaction chamber, particularly the reaction site, and is governed by the system geometry. The average linear gas stream velocity is typically computed in a hot wall system to provide a normalization of the geometry (33). However, it is practically very difficult to get a meaningful value of the linear gas stream velocity in a cold wall system due to the complex reactor geometry. In this work, flow rates are used for analysis, instead of linear gas stream velocities.

The residence time of the input gas in a reactor is defined as $t = 60 VP/f$, where $t = 3$ residence time (s), $V =$ volume of the reactor (liters), $f =$ flow rate (SLPM), $P =$ pressure (atm). At a low flow rate, the residence time of the reactant introduced into the reaction chamber may be long in comparison to chemical reaction or mass-transfer rates. Hence the chemical system in the reactor may be expected to approach equilibrium. Once the system approaches equilibrium, the input gas flow rate becomes the mass transport rate. In other words, in this regime the deposition rate is determined entirely by the input gas flow rate, and therefore is proportional to the flow rate. In Fig. 13 the deposition rate is a linear function of the flow rate.

On the other hand, as the reactants flow along the length of the reaction chamber, a portion of the reactant gas is consumed. The partial pressure of the reactant gas is thus lower near the outlet end of the reactor, and the deposition rate is reduced there if all other deposition parameters remain constant. The calculated residence time for the system used here is shown in Table II. As can be seen in the table, the residence time increases as the flow rate decreases. When the flow rate or gas stream velocity is low,

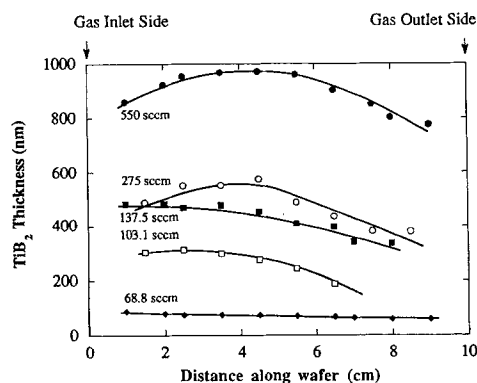


Fig. 14. The thickness of TiB_2 as a function of location on the wafer for various flow rates. The films were deposited at $600^\circ C$, $B/B + Ti = 0.67$, and 1 torr.

Table II. The residence time at various input gas flow rates at $600^\circ C$, 1 torr, $B/B + Ti = 0.67$.

Flow rate (sccm)	68.8	103.1	137.5	275	550
Residence time (s)	21.9	14.7	11.0	5.5	2.8

i.e., the residence time is long, depletion of input gases might be expected to occur. Indeed, as can be seen in Fig. 14, for total flow rates below 137.5 sccm the thickness of TiB_2 decreases along the direction of gas travel, indicating depletion of the input gas, while at high flow rates with short residence times, the thickness is maximum at the center of the wafer and decreases radially. The location of the maximum thickness is observed to shift from the wafer edge nearest the gas injector to that of the pumping port as the flow rate (linear gas stream velocity) increases. This is probably because that it takes longer for the input gas to approach the deposition temperature at high flow rate. Even though the numerical results are reactor specific, the general trends should be applicable to a range of cold wall systems.

The effect of pressure on deposition.—A series of experiments to study the dependence of pressure on deposition of TiB_2 were performed. The total pressure of the chamber was varied from 0.1 to 4 torr by throttling the exhaust valve. The other deposition variables were fixed at $600^\circ C$, 250 sccm total flow rate having $B/B + Ti = 0.67$ and 6 min deposition time. Figure 15 shows the dependence of the deposition rate of TiB_2 films on the total pressure. No deposition was detected at 0.1 torr, even using four-point probe sheet resistance measurement, which should be sensitive to the presence of an ultra thin film. A meaningful value of deposition rate could not be obtained at a pressure of 4 torr due to poor thickness uniformity. As can be seen in the figure, the deposition rate linearly increases with the input partial pressure of $TiCl_4$ and B_2H_6 . The film thickness variation on the wafer along the direction of gas flow is plotted in Fig. 16, where evidence of gas depletion is seen above 1 torr. The location of the maximum in the film thickness shifts from the leading (input) to the trailing (exhaust) edge as the pressure decreases from 2 to 0.5 torr.

For a horizontal CVD reactor, the boundary layer thickness, δ , can be determined using the equation: $\delta = (D_r d / Re)^{1/2}$, where D_r is the diameter of the tube, d is the axial distance along the tube, and Re is the Reynolds number. Evidently D_r and d are independent of the pressure. The Reynolds number is calculated using the formula: $Re = D_d \times L / D_A$, where D_d is linear gas stream velocity, L is a characteristic length descriptive of the flow field which, for the case of gas flow in a tube, would be equal to the diameter of the tube, and D_A is diffusion constant. Because L is independent of pressure and both the linear gas stream velocity and the diffusion constant are inversely proportional to the system pressure, the Reynolds number and consequently boundary layer thickness are independent of the pressure (34). However the deposition rate increases

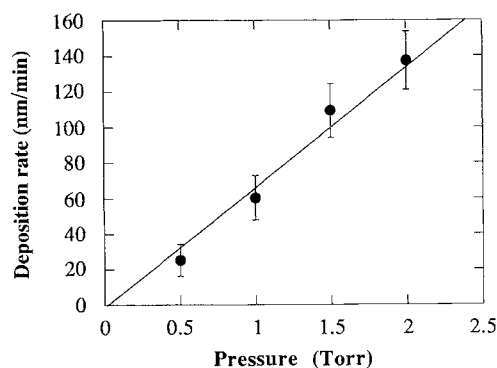


Fig. 15. Deposition rate as a function of deposition pressure. The deposition rate increases linearly with pressure. The depositions were performed at $B/B + Ti = 0.67$, $600^\circ C$.

Table III. The residence time and deposition efficiency at various pressures at 600°C, 275 sccm total flow, B/B + Ti = 0.67.

Total pressure (torr)	0.5	1.0	1.5	2.0
Residence time (s)	2.8	5.5	8.2	11.0
Deposition efficiency (%)	0.75	8.1	13.5	18

linearly with the partial pressure of the reactants, which is proportional to total pressure in this experiment.

The residence time of the input gas in the chamber and deposition efficiency are calculated in Table III. The deposition efficiency is defined as a ratio of the mole amount of Ti deposited on the heated area to the mole amount of Ti in the input gas based on the input gas flow rate. The residence time of reactant and the deposition efficiency both increase with the pressure. The gas depletion effect discussed earlier in the flow rate experiments is observed again in these pressure experiments for long residence times.

At the total pressure of 2 torr where the residence time is 11 s, the input gas depletion effect is very pronounced, *i.e.*, the film thickness on the wafer decreases along the direction of gas flow. A more uniform wafer, having the thickest film more symmetrically at the center, is obtained at the pressure of 1 torr. It is very interesting to note the shift of the thickest film position from the front of the wafer at 2 torr toward the back at 0.5 torr, presumably caused by the low pressure gas taking longer (traveling farther) to achieve thermal equilibrium.

Roughness of the films.—The surface of the films were scanned with a Dektak profilometer to measure the roughness of the film. In Fig. 17 the roughness of the films represented by the height difference between peaks and valleys is shown as a function of the film thickness. This figure contains two different variables: varying the deposition time from 1 to 6 min or varying the flow rate from 68.75 to 550 sccm, keeping the other process conditions constant. The deposition condition was 600°C, 1 torr, 6 min, and 275 sccm of input flow rate with B/B + Ti = 0.67. The agreement of both sets of data suggests that the surface roughness of the films is independent of the total flow rate, increases linearly with the film thickness, and typically amounts to about 5%.

Conformal deposition.—One advantage of chemical vapor deposition is its conformality. The film deposited over a 0.5 μm wet-etched oxide step at 600°C, 1 torr, B/B + Ti = 0.67 shows a conformal deposition. The film thickness on the etched wall and bottom is more than 90% of that on top of the step. This result indicates good conformal coverage of TiB₂ over moderate steps.

Etching.—TiB₂ films deposited on thermal silicon dioxide at 600°C and above were wet etched in 30% H₂O₂ at room temperature. Wet etching in H₂O₂ left a very thin layer (<10 nm measured by XPS) on the etched surface. Because the thickness of the unetched layer was very thin, the use of chemical analysis to verify the content of the

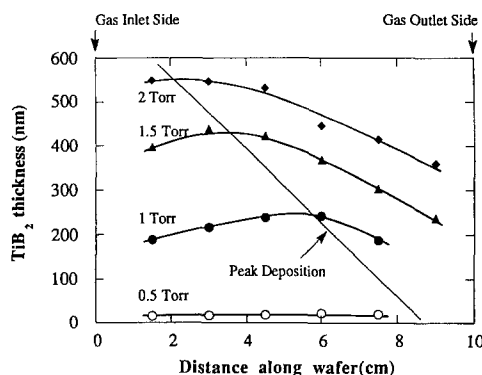


Fig. 16. The thickness of TiB₂ as a function of location in the wafer for various pressures. The films were deposited at 600°C, B/B + Ti = 0.67, and 275 sccm total flow rate.

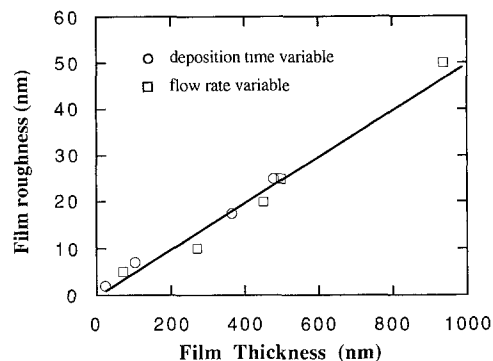


Fig. 17. The roughness of TiB₂ films as a function of film thickness.

film was very difficult. However, the thermodynamic analysis discussed earlier suggested that an interface layer between the substrate and the TiB₂ film would be present. Boron oxide and titanium oxide are expected to form on a silicon dioxide substrate while titanium silicide is predicted on a Si substrate. The presence of such a residual layer leads to a high level of leakage currents between adjacent TiB₂ dots which are defined by photolithography, and hindered any further meaningful electrical measurements. The remaining residue from the TiB₂ films on an SiO₂ substrate could be etched in a single-wafer, magnetically enhanced plasma reactor (35). For the dry etching, CF₂Cl₂ was initially used for a very short period of time to nonselectively etch any surface materials. Subsequently Br₂ was used for the main part of the etch because it is well known to give highly anisotropic profiles with a very high selectivity to the underlying oxide. The electrical measurements on dry etched TiB₂ film suggested that dry etching with such a combination of reactants successfully etched TiB₂ films on thermal oxide.

Conclusions

A thermodynamic analysis of the chemical vapor deposition of TiB₂ from gaseous TiCl₄, B₂H₆, and H₂ was performed using SOLGASMIX and served as a guide line for selecting process conditions. In TiCl₄-rich gas mixtures, multiphase deposits of titanium silicides and titanium diboride are predicted on a silicon substrate. In a diborane-rich input gas mixture, elemental boron is expected to accompany TiB₂ deposition on a silicon substrate. However, at an input gas ratio corresponding to the stoichiometry of TiB₂, the amount of secondary-phase deposition is predicted to be considerably reduced compared to that of TiB₂. On the other hand, in addition to TiB₂, titanium oxide and boron oxides are expected to deposit on SiO₂ substrates in a TiCl₄-rich gas mixture, while boron and titanium diboride are expected in a B₂H₆-rich gas mixture. To take advantage of the widest single-phase window possible for both substrates, the thermodynamically optimized standard condition for input gas mixture and deposition temperature were chosen as B/B + Ti = 0.67 and 600°C, respectively. Multiple-phase deposition is predicted on most other substrates.

X-ray diffraction data indicated the presence of a very fine grained polycrystalline or amorphous phase for as-deposited films. However, the films RTA-annealed above 900°C gave patterns corresponding to the TiB₂ structure. Except for an oxidized layer at the surface, the films appear to be pure TiB₂ when analyzed via XPS.

The film thickness increased linearly with the growth time, and the deposition rate was independent of the substrate (Si vs. SiO₂). Two distinct regimes of deposition kinetics were evident in different deposition temperature ranges. Below 600°C, surface reactions are found to be the dominant factor for the kinetics of TiB₂ deposition, while mass transport is the limiting step for deposition above 600°C. Activation energies for deposition were determined to be 1.36 eV, and 0.31 eV for low and high temperature deposition, respectively. The presence of excess boron and chlorine was detected throughout the bulk for low-temperature films. As the deposition temperature increased,

the B/Ti ratio approached the stoichiometric value of two, and remained constant at higher temperatures; furthermore the Cl content was reduced. Over a wide range of input gas mixture ratios from 0.4 to 0.71, the films were found to have a constant, nearly stoichiometric B/Ti ratio. This result indicates that the window to deposit single-phase TiB₂ is quite wide. The peak in deposition rate was found to occur close to an input gas ratio corresponding to stoichiometry (0.67), suggesting that the deposition mechanism was reactant limited. The deposition rate increased linearly with flow rate and pressure, indicating that the mechanism for deposition was equilibrium limited in the range of flow rate 70-550 sccm. Input gas depletion effects were observed at low flow rates and high pressures where the residence time of reactants was longer than 10 s. A surface reaction limited mechanism was not observed in these experiments, even at the maximum flow rate of 550 sccm. The roughness of the films increased linearly with the thickness.

To get stoichiometric and uniform films in the reactor used in this study, the optimized process condition was 600°C, 1 torr, total flow rate of 550 sccm with an input gas mixture of B/B + Ti = 0.67.

Acknowledgments

This work has been supported by the Semiconductor Research Corporation (Contract No. 89-MP-132) and MCNC. The authors also gratefully acknowledge helpful discussion with A. Reisman, and J. J. Wortman of the Nanometer Engineering Laboratory of NCSU/MCNC and Stephen Bobbio at MCNC. They would like to thank C. U. Ro, A. S. Shah, Susan K. Hofmeister, and J. D. Hunn for technical assistance.

Manuscript submitted Feb. 25, 1991; revised manuscript received May 6, 1991. This was Paper 313 presented at the Washington, DC, Meeting of the Society, May 5-10, 1991.

North Carolina State University assisted in meeting the publication costs of this article.

REFERENCES

- K. K. Ng and W. T. Lunch, *IEEE Trans. Electron Devices*, **ED-34**, 503 (1987).
- S. P. Murarka, "Silicides for VLSI Applications," Academic Press, Inc., New York (1983).
- M.-A. Nicolet, *Thin Solid Films*, **52**, 415 (1978).
- G. V. Samsonov, B. A. Kovenskaya, and T. I. Serebryakova, *Izv. Vyssh. Ucheb. Zaved. Fiz.*, **14**, 19 (1971).
- A. D. McLeod, J. S. Haggerty, and D. R. Sadoway, *J. Am. Ceram. Soc.*, **67**, 705 (1984).
- J. R. Shappirio, J. J. Finnegan, and R. A. Lux, *J. Vac. Sci. Technol. A*, **3**, 2255 (1985).
- C. Feldman, F. G. Satkiewicz, and N. A. Blum, *J. Less-Common Met.*, **82**, 183 (1981).
- J. G. Ryan, S. Roberts, G. J. Slusser, and E. D. Adams, *Thin Solid Films*, **153**, 329 (1982).
- T. Shikama, Y. Sakai, M. Fukutomi, and M. Okada, *ibid.*, **156**, 287 (1988).
- T. Shikama, Y. Sakai, M. Fujitsuka, Y. Tamauchi, H. Shinno, and M. Okada, *ibid.*, **164**, 95 (1988).
- T. Larsson, H.-O. Blom, S. Berg, and M. Östling, *ibid.*, **172**, 133 (1989).
- H.-O. Blom, T. Larsson, S. Berg, and M. Östling, *J. Vac. Sci. Technol. A*, **6**, 1693 (1988).
- T. Sato, M. Kudo, and T. Tachikawa, *Denki Kagaku*, **55**, 542 (1987).
- J. D. Casey and J. S. Haggerty, *J. Mater. Sci.*, **22**, 737 (1987).
- C. Feldman, F. G. Satkiewicz, and G. Jones, *J. Less-Common Met.*, **79**, 221 (1981).
- P. Peshev and T. Niemyski, *ibid.*, **10**, 133 (1965).
- R. E. Gannon, R. C. Folweiler, and T. Vasilos, *J. Am. Ceram. Soc.*, **46**, 496 (1963).
- J. J. Gebhart and R. F. Cree, *ibid.*, **48**, 262 (1965).
- T. M. Besmann and K. E. Spear, *This Journal*, **124**, 790 (1977).
- H. O. Pierson and A. W. Mullendore, *Thin Solid Films*, **95**, 99 (1982).
- E. Randich and T. M. Gerlach, *ibid.*, **75**, 271 (1981).
- L. W. William, *Appl. Phys. Lett.*, **46**, 43 (1985).
- H. O. Pierson and A. W. Mullendore, *Thin Solid Films*, **72**, 511 (1980).
- "CRC Hand Book of Chemistry and Physics," R. C. Weast, Editor (1985-1986).
- C. S. Choi, G. C. Xing, G. A. Ruggles, C. M. Osburn, A. S. Shah, and J. D. Hunn, in "ULSI Science and Technology/1991," J. M. Andrews and G. K. Celler, Editors, PV 91-11, p. 343, The Electrochemical Society Softbound Proceedings Series, Pennington, NJ (1991).
- C. S. Choi, G. A. Ruggles, C. M. Osburn, and G. C. Xing, *J. Appl. Phys.*, **69**, 7853 (1991).
- C. Choi, G. A. Ruggles, C. M. Osburn, P. Shea, and G. S. Xing, in "Proceeding of MRS Symposium, Advanced Metallization in Microelectronics," Vol. 181, 455 (1990).
- T. M. Besmann and K. E. Spear, *This Journal*, **124**, 790 (1977).
- R. J. H. Clark, "The Chemistry of Titanium and Vanadium," p. 40, Elsevier Pub. Co., New York (1968).
- N. Nakanishi, S. Mori, and E. Kato, *This Journal*, **137**, 322 (1990).
- G. J. Reynolds, C. B. Cooper III, and P. J. Gaczi, *J. Appl. Phys.*, **65**, 3213 (1989).
- A. Bouteville, A. Royer, and J. C. Remy, *This Journal*, **134**, 2080 (1987).
- A. Reisman and M. Berkenblit, *ibid.*, **113**, 146 (1966).
- A. Reisman, Private communication.
- S. Bobbio and Y. Ho, U.S. Pat. 4,738,761 (1988).